



Cite this: DOI: 10.1039/c5cc01211b

Received 9th February 2015,  
Accepted 19th March 2015

DOI: 10.1039/c5cc01211b

www.rsc.org/chemcomm

# A pH-switched Pickering emulsion catalytic system: high reaction efficiency and facile catalyst recycling†

Jianping Huang and Hengquan Yang\*

A smart Pickering emulsion catalytic system is constructed, which not only exhibits fivefold reaction rate enhancement effects in comparison to the conventional biphasic system but also can be facilely demulsified by tuning pH, allowing for *in situ* recycling nanocatalysts.

The organic/aqueous biphasic catalytic system is an important platform for many chemical transformations such as hydroformylation, biocatalysis and biomass refining.<sup>1</sup> Despite their wide range of applications, biphasic systems often suffer from low reaction efficiency due to high mass transfer resistance.<sup>2</sup> To overcome this obstacle, co-solvents, phase-transferable reagents<sup>3</sup> and thermoregulated biphasic systems are employed or explored.<sup>4</sup> These methods, however, require the introduction of extra additives or relatively complicated procedures to modify catalysts.

In parallel, recent years have witnessed that nanoparticle catalysts gain unprecedented popularity due to their unique properties.<sup>5</sup> Their practical applications, however, are usually hindered by notorious difficulty in separation and recycling.<sup>6</sup> Although magnetic-field-assisted separation, ultrafiltration, and high-speed centrifugation have been developed to address these issues,<sup>7</sup> these approaches require external magnetic fields or transferring the reaction mixture from the reaction vessel to other vessels. In this context, alternative methods to efficiently recycle nanoparticle catalysts are highly desired.

To address the above two issues our group has recently developed a pH-triggered Pickering emulsion (particle-stabilized) inversion system and a Pickering emulsion/organic biphasic system.<sup>8</sup> These systems along with other studies exhibit high reaction efficiency due to the large reaction interface area.<sup>9</sup> However, only a fraction of the organic product can be separated at the end of reaction because other fractions are sacrificed in the Pickering emulsion phase. We envision that more organic

products would be separated if Pickering emulsion could be broken. However, detaching a nanoparticle from the droplet surface needs to overcome an energy barrier that is several orders of magnitude higher than its thermal energy.<sup>10</sup> To further address this challenge, herein we first demonstrate a smart Pickering emulsion catalytic system that can be demulsified at the end of reaction. As shown in Fig. 1, using appropriate, pH-responsive nanoparticle catalysts (Fig. 1a), one can transfer a conventional biphasic system to a water-in-oil (W/O) Pickering emulsion system in the beginning of reaction (Fig. 1b). At the end of reaction, this Pickering emulsion system is demulsified by adding acid and macroscopic phase separation therefore occurs. The organic phase can be isolated through simple liquid transfer whilst the catalyst-contained water can be directly used for the next reaction cycle after tuning the pH.

The key for this strategy is to obtain smart nanoparticle catalysts that can disassemble at the oil/water interface on command. Thermal and magnetic triggers have reported to break emulsion, yet require high temperature or sufficiently strong magnetic field to overcome the high energy barrier.<sup>11</sup> In contrast, pH may be a good candidate because it can alter the catalyst surface wettability as so to promote effective demulsification.

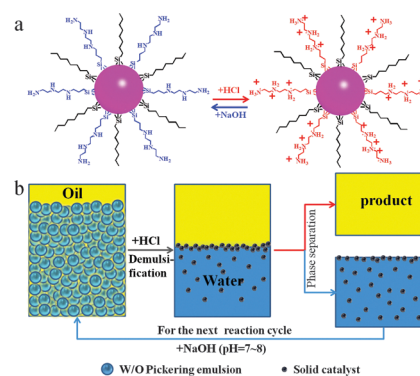


Fig. 1 Schematic illustration of the pH-switched Pickering emulsion strategy. (a) Protonation-deprotonation of a nanoparticle catalyst. (b) Demulsification, organic product separation and catalyst recycling.

School of Chemistry and Chemical Engineering, Shanxi University,  
Wucheng Road 92, Taiyuan 030006, China. E-mail: hqyang@sxu.edu.cn

† Electronic supplementary information (ESI) available: Experimental section; N<sub>2</sub> sorption analysis; TEM images; EELS mapping; solid state NMR spectra; EDS spectrum. See DOI: 10.1039/c5cc01211b

Although pH-responsive polymer emulsifiers are available in the literature,<sup>12</sup> inorganic particles are preferred because of its robustness. As extension to our previous protocol,<sup>8</sup> we here used a significantly increased molar fraction of pH sensitive (MeO)<sub>3</sub>SiCH<sub>2</sub>CH<sub>2</sub>CH<sub>2</sub>(NHCH<sub>2</sub>CH<sub>2</sub>)<sub>2</sub>NH<sub>2</sub> (10%, in its mixture with hydrophobic (MeO)<sub>3</sub>Si(CH<sub>2</sub>)<sub>7</sub>CH<sub>3</sub>) to modify smaller silica nanospheres. The obtained material is denoted as SN-ON. For comparison, we also prepared triamine-monofunctionalized and octyl-monofunctionalized silica microspheres, denoted as SN-N and SN-O, respectively.

The TEM image shows that SN-ON consists of monodisperse spheres with diameters of around 50–60 nm (Fig. S1a, ESI†). It is almost non-porous since its specific surface area is only 37 m<sup>2</sup> g<sup>−1</sup> (Fig. S2, ESI†). The electron energy loss energy (EELS) confirms that triamine and octyl groups are both uniformly distributed on silica nanospheres (Fig. S1b, ESI†). The solid state <sup>13</sup>C CP-MAS NMR spectrum exhibits C signals, which can be assigned to octyl and triamine groups (Fig. S3a, ESI†). In the solid state <sup>29</sup>Si CP-MAS NMR spectrum (Fig. S3b, ESI†), T<sup>3</sup> [SiR(OSi)<sub>3</sub>] and T<sup>2</sup> [SiR(OSi)<sub>2</sub>(OH)] bands appear, indicating that these functionalities are linked to the SiO<sub>2</sub> surface through Si–O–Si bonds. Elemental analysis gives quantitative results (Table S1, ESI†): octyl and triamine loadings on SN-ON are 0.31 and 0.12 mmol g<sup>−1</sup>, respectively; the octyl loading on SN-O 0.31 mmol g<sup>−1</sup>; triamine loading on SN-N 0.72 mmol g<sup>−1</sup>. These results are broadly supported by the TG measurement result (Fig. S4, ESI†).

After mixtures of silica nanospheres, ethyl acetate and water were stirred for 3 min (800 rpm), different phenomena were observed (Fig. 2). For SN-O and SN-N, the systems consist of two phases with SN-O and SN-N distributed in the upper oil phase and the lower water phase, and emulsion droplets were not found using an optical microscope. Different from SN-O and SN-N, SN-ON led to a Pickering emulsion phase at the bottom since droplets were observed. The drop test confirmed that it was of W/O type. Interestingly, after adding a few drops of HCl solution, the systems with SN-O and SN-N had no obvious changes, while the SN-ON-stabilized Pickering emulsion was demulsified, as observed from the optical micrographs. When a few drops of NaOH solution were added and the pH was tuned

to 7–8, the system with SN-ON rapidly restored Pickering emulsion. Moreover, this reversible switch behaviour was observed in other biphasic systems such as toluene-, benzene-, ether-, dichloromethane- and trichloromethane–water (Fig. S5, ESI†). More impressively, the SN-ON-stabilized Pickering emulsion could be reversibly switched on and off at least ten times (Fig. S6, ESI†). The significantly different behaviour of these materials is attributed to the difference in surface chemistry. SN-O and SN-N are too hydrophobic or too hydrophilic to stabilize Pickering emulsion, whereas SN-ON is not only moderately hydrophobic but also pH-responsive. After the SN-ON surface triamines are protonated, their surfaces become too hydrophilic to stabilize emulsion.

Next, hydrogenation was chosen to evaluate the catalytic efficiency and recyclability. We prepared a Pd/SN-ON by loading Pd nanoparticles on SN-ON (Pd loading is 1 wt%). The TEM image shows that Pd nanoparticles (1–2 nm in size) are homogeneously distributed on the surface (Fig. S7a, ESI†). X-ray (EDX) spectroscopy (EDS) confirms the presence of Pd besides N, C, O and Si elements (Fig. S7b, ESI†).

We compared Pd/SN-ON catalytic efficiency in the Pickering emulsion system and in the conventional biphasic system that was obtained by adding isopropyl alcohol as the demulsifier. Based on H<sub>2</sub> consumption rates (Fig. 3a), one can find that these two systems proceeded at remarkably different rates. Fig. 3b quantitatively compares their catalytic efficiency (CE, see the footnote of Fig. 3). CE in the Pickering emulsion is 5.14 times higher than that in the conventional biphasic. The significantly enhanced catalytic efficiency is attributed to the presence of emulsion droplets that create a large reaction interface area. At the end of reaction, the Pickering emulsion was demulsified after lowering the pH to 3–4, allowing the organic product to separate through a simple liquid decantation (Fig. 3c and Fig. S8, ESI†). In the subsequent reaction cycles, Pickering emulsion was obtained again by increasing the pH to 7–8. As shown in Fig. 3e, ethylbenzene yield is up to 83% in the first reaction, which is higher than those obtained with our previous Pickering emulsion systems.<sup>8</sup> From the second to fifth cycle, all isolated yields are more than 90%. The slight activity loss is due to the Pd particle aggregation and slight Pd leaching (Fig. S9, ESI†).

This smart system worked well for hydrogenation of other unsaturated compounds. Table 1 lists the results for the first and second reaction cycles. For all the investigated substrates, Pickering emulsion systems gave more than 98% conversions within 1.5–3 h, and 77–82% yields can be achieved with a little amount of product sacrificed at the phase boundary (Fig. S7, ESI†). In the second reaction cycle, 99% conversions were afforded and the yields increased up to 97–99%. The results further justify the importance of our smart Pickering emulsion strategy.

In summary, through appropriate surface modification we first demonstrate a pH-responsive Pickering emulsion system for organic/aqueous biphasic catalysis. Such a system exhibits fivefold reaction rate enhancement effects in comparison to the conventional biphasic reaction. Its demulsification on

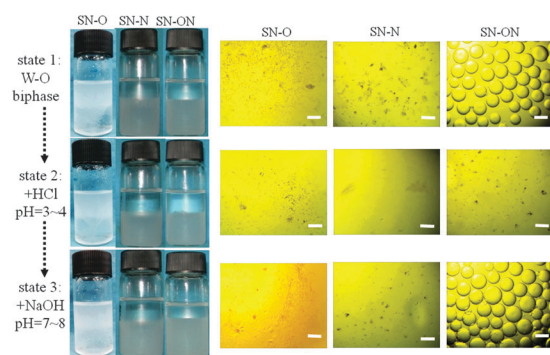
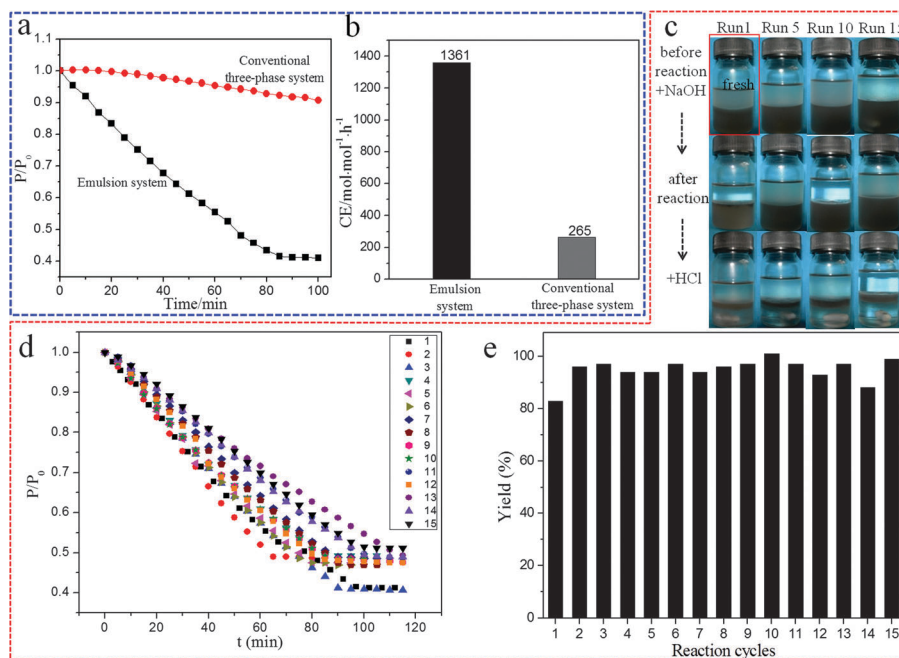
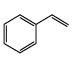
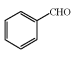
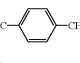
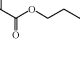
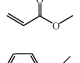
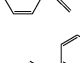
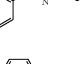
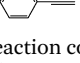


Fig. 2 Appearance of ethyl acetate–water mixture in the presence of different silica nanospheres (photographs taken after standing for 0.5 h). Every vial contains 4 mL of ethyl acetate, 4 mL of water, and 0.04 g of silica nanospheres. State 1: before adding HCl (1 M); state 2: pH is adjusted to 3–4 using HCl; state 3: pH is adjusted to 7–8 using NaOH (1 M). Scale bar is 200 μm.



**Fig. 3** Results of styrene hydrogenation in the Pickering emulsion and the conventional biphasic. (a)  $H_2$  consumption curves. (b) Catalytic efficiency (CE) (CE = moles of the converted substrate/Pd moles  $\times$  reaction time h). (c) Photographs for selected reaction cycles. Before reaction, the pH value is adjusted to 7–8 except Run 1; after reaction, the pH value is adjusted to 3–4 to demulsify. (d)  $H_2$  consumption curves for fifteen reaction cycles. (e) Ethylbenzene yields for fifteen reaction cycles. Reaction conditions: 5.6 mL of water, 5.6 mL of ethyl acetate, 56 mg of Pd/SN-ON, 1.1054 g of styrene ( $S/C = 2000$ ), 40 °C, 0.35 MPa, 800 rpm. Conventional biphasic system used 1.6 mL of isopropyl alcohol and 4 mL of water as the aqueous phase.

**Table 1** Results of the hydrogenation of various substrates in Pickering emulsion systems

Substrates	Run 1			Run 2		
	Time (h)	Conv. (%)	Yield (%)	Time (h)	Conv. (%)	Yield (%)
 <sup>a</sup>	1.5	> 99	83	1.2	> 99	96
 <sup>b</sup>	3	98	81	5	> 99	99
 <sup>b</sup>	3	> 99	78	5	> 99	99
 <sup>c</sup>	1.5	> 99	81	1.5	> 99	98
 <sup>c</sup>	1.5	> 99	82	1.5	> 99	98
 <sup>c</sup>	1.5	> 99	82	1.5	> 99	98
 <sup>d</sup>	3	> 99	82	3	> 99	100
 <sup>d</sup>	2.5	> 99	77	2.5	> 99	97

Reaction conditions. <sup>a</sup> 5.6 mL of water, 5.6 mL of ethyl acetate, 56 mg of Pd/SN-ON and a certain amount of substrate and stirring at 800 rpm. 40 °C, 0.35 MPa,  $S/C = 2000$ . <sup>b</sup> 5.6 mL of water, 5.6 mL of ethyl acetate, 56 mg of Pd/SN-ON and a certain amount of substrate and stirring at 800 rpm. 50 °C, 2 MPa,  $S/C = 1000$ . <sup>c</sup> 5.6 mL of water, 5.6 mL of ethyl acetate, 56 mg of Pd/SN-ON and a certain amount of substrate and stirring at 800 rpm. 40 °C, 2 MPa,  $S/C = 1000$ . <sup>d</sup> 2 mL of water, 2 mL of ethyl acetate, 20 mg of Pd/SN-ON,  $S/C = 1000$ , 800 rpm, 40 °C,  $H_2$  2 MPa.

command not only enables the facile separation of organic products but also allows the nanocatalysts to be “*in situ*” recycled at least 15 times.

We acknowledge the Natural Science Foundation of China (221173137), program for New Century Excellent Talents in University (NECT-12-1030) and Program for Middle-aged Innovative Talents of Higher Learning Institutions of Shanxi (20120202).

## Notes and references

- (a) W. Keim, *Green Chem.*, 2003, 5, 105; (b) P. Pollet, R. J. Hart, C. A. Eckert and C. L. Liotta, *Acc. Chem. Res.*, 2010, 43, 1237.
- (a) C. J. Li and L. Chen, *Chem. Soc. Rev.*, 2006, 35, 68; (b) S. Minakata and M. Komatsu, *Chem. Rev.*, 2009, 109, 711.
- T. Hashimoto and K. Maruoka, *Chem. Rev.*, 2007, 107, 5656.
- C. Liu, X. M. Li and Z. L. Jin, *Catal. Today*, 2015, 247, 82.
- D. Astruc, F. Lu and J. R. Aranzas, *Angew. Chem., Int. Ed.*, 2005, 44, 7852.
- (a) S. Shylesh, V. Schnemann and W. R. Thiel, *Angew. Chem., Int. Ed.*, 2010, 49, 3428; (b) X. H. Li, W. L. Zheng, H. Y. Pan, Y. Yu, L. Chen and P. Wu, *J. Catal.*, 2013, 300, 9.
- S. Shylesh, V. Schunemann and W. R. Thiel, *Angew. Chem., Int. Ed.*, 2010, 49, 3428.
- (a) H. Q. Yang, T. Zhou and W. J. Zhang, *Angew. Chem., Int. Ed.*, 2013, 52, 7455; (b) H. F. Liu, Z. M. Zhang, H. Q. Yang, F. Q. Cheng and Z. P. Du, *ChemSusChem*, 2014, 7, 1888.
- (a) S. Crossley, J. Faria, M. Shen and D. E. Resasco, *Science*, 2010, 327, 68; (b) W. J. Zhang, L. M. Fu and H. Q. Yang, *ChemSusChem*, 2014, 7, 391; (c) L. M. Fu, S. R. Li, Z. Y. Han, H. F. Liu and H. Q. Yang, *Chem. Commun.*, 2014, 50, 10045; (d) Z. W. Chen, L. Zhou, W. Bing, Z. J. Zhang, Z. H. Li, J. S. Ren and X. G. Qu, *J. Am. Chem. Soc.*, 2014, 136, 7498; (e) W. J. Zhou, L. Fang, Z. Y. Fan, B. Albela, L. Bonnevot, F. D. Campo, M. P. Titus and J. M. Clacens, *J. Am. Chem. Soc.*, 2014, 136, 4869; (f) H. Q. Yang, L. M. Fu, L. J. Wei, J. F. Liang and

- B. P. Binks, *J. Am. Chem. Soc.*, 2015, **137**, 1362; (g) H. Y. Tan, P. Zhang, L. Wang, D. Yang and K. B. Zhou, *Chem. Commun.*, 2011, **47**, 11903; (h) Z. P. Wang, M. C. M. van Oers, F. P. J. T. Rutjes and J. C. M. van Hest, *Angew. Chem., Int. Ed.*, 2012, **51**, 10746; (i) L. Leclercq, R. Company, A. Mühlbauer, A. Mouret, J. M. Aubry and V. Nardello-Rataj, *ChemSusChem*, 2013, **6**, 1533; (j) M. Li, D. C. Green, J. L. Ross Anderson, B. P. Binks and S. Mann, *Chem. Sci.*, 2011, **2**, 1739; (k) Z. W. Chen, H. W. Ji, C. Q. Zhao, E. G. Ju, J. S. Ren and X. G. Qu, *Angew. Chem., Int. Ed.*, 2015, **54**, DOI: 10.1002/anie.201412049; (l) M. Pera-Titus, L. Leclercq, J. Clacens, F. D. Campo and V. Nardello-Rataj, *Angew. Chem., Int. Ed.*, 2015, **54**, 2006; (m) J. Liu, G. J. Lan, J. Peng, Y. Li, C. Li and Q. H. Yang, *Chem. Commun.*, 2013, **49**, 9558; (n) Z. Zheng, J. L. Wang, H. L. Chen, L. B. Feng, R. Jing, M. Z. Lu, B. Hu and J. B. Ji, *ChemCatChem*, 2014, **6**, 1626; (o) Y. H. Yu, L. M. Fu, F. W. Zhang, T. Zhou and H. Q. Yang, *ChemPhysChem*, 2014, **15**, 841.
- 10 K. Du, E. Glogowski, T. Emrick, T. P. Russell and A. D. Dinsmore, *Langmuir*, 2010, **26**, 12518.
  - 11 (a) Y. D. Wu, S. Wiese, A. Balaceanu, W. Richtering and A. Pich, *Langmuir*, 2014, **30**, 7660; (b) J. Zhou, X. Qiao, B. P. Binks, K. Sun, M. Bai, Y. Li and Y. Liu, *Langmuir*, 2011, **27**, 3308.
  - 12 (a) A. J. Morse, D. Dupin, K. L. Thompson, S. P. Armes, K. Ouzineb, P. Mills and R. Swart, *Langmuir*, 2012, **28**, 11733; (b) K. Geisel, L. Isa and W. Richtering, *Angew. Chem., Int. Ed.*, 2014, **53**, 4905; (c) J. H. Sun, C. L. Yi, W. Wei, D. H. Zhao, Q. Hu and X. Y. Liu, *Langmuir*, 2014, **30**, 14757.